Video Article

Harvesting Solar Energy by Means of Charge-Separating Nanocrystals and Their Solids

Geoffrey Diederich[1], Timothy O'Connor[1], Pavel Moroz[2,3], Erich Kinder[1], Elena Kohn[2,3], Dimuthu Perera[1], Ryan Lorek[1], Scott Lambright[1], Martene Imboden[3], Mikhail Zamkov[1,2]

[1]Department of Physics, Bowling Green State University

[2]The Center for Photochemical Sciences, Bowling Green State University

[3]Department of Chemistry, Bowling Green State University

Correspondence to: Mikhail Zamkov at zamkovm@bgsu.edu

URL: https://www.jove.com/video/4296
DOI: doi:10.3791/4296

Keywords: Physics, Issue 66, Materials Science, Chemical Engineering, Chemistry, Electrical Engineering, Photovoltaics, nanorods, dye-sensitized, solids, titanium dioxide, photocatalysis, quantum dots

Date Published: 8/23/2012

Citation: Diederich, G., O'Connor, T., Moroz, P., Kinder, E., Kohn, E., Perera, D., Lorek, R., Lambright, S., Imboden, M., Zamkov, M. Harvesting Solar Energy by Means of Charge-Separating Nanocrystals and Their Solids. *J. Vis. Exp.* (66), e4296, doi:10.3791/4296 (2012).

Abstract

Conjoining different semiconductor materials in a single nano-composite provides synthetic means for the development of novel optoelectronic materials offering a superior control over the spatial distribution of charge carriers across material interfaces. As this study demonstrates, a combination of donor-acceptor nanocrystal (NC) domains in a single nanoparticle can lead to the realization of efficient photocatalytic[1-5] materials, while a layered assembly of donor- and acceptor-like nanocrystals films gives rise to photovoltaic materials.

Initially the paper focuses on the synthesis of composite inorganic nanocrystals, comprising linearly stacked ZnSe, CdS, and Pt domains, which jointly promote photoinduced charge separation. These structures are used in aqueous solutions for the photocatalysis of water under solar radiation, resulting in the production of H_2 gas. To enhance the photoinduced separation of charges, a nanorod morphology with a linear gradient originating from an intrinsic electric field is used[5]. The inter-domain energetics are then optimized to drive photogenerated electrons toward the Pt catalytic site while expelling the holes to the surface of ZnSe domains for sacrificial regeneration (via methanol). Here we show that the only efficient way to produce hydrogen is to use electron-donating ligands to passivate the surface states by tuning the energy level alignment at the semiconductor-ligand interface. Stable and efficient reduction of water is allowed by these ligands due to the fact that they fill vacancies in the valence band of the semiconductor domain, preventing energetic holes from degrading it. Specifically, we show that the energy of the hole is transferred to the ligand moiety, leaving the semiconductor domain functional. This enables us to return the entire nanocrystal-ligand system to a functional state, when the ligands are degraded, by simply adding fresh ligands to the system[4].

To promote a photovoltaic charge separation, we use a composite two-layer solid of PbS and TiO_2 films. In this configuration, photoinduced electrons are injected into TiO_2 and are subsequently picked up by an FTO electrode, while holes are channeled to a Au electrode via PbS layer[6]. To develop the latter we introduce a *Semiconductor Matrix Encapsulated Nanocrystal Arrays* (SMENA) strategy, which allows bonding PbS NCs into the surrounding matrix of CdS semiconductor. As a result, fabricated solids exhibit excellent thermal stability, attributed to the heteroepitaxial structure of nanocrystal-matrix interfaces, and show compelling light-harvesting performance in prototype solar cells[7].

Video Link

The video component of this article can be found at https://www.jove.com/video/4296/

Protocol

1. Synthesis of ZnSe Core Nanocrystals[8]

1. Place 7.0 g ODA and a magnetic stir bar into a three neck flask.
2. In a separate flask, combine 0.063 g Se and 2.4 ml TOP and add a magnetic stir bar. The mixture of TOP and selenium should be degassed under vacuum for 30 min.
3. Degas ODA for 90 min at 120 °C, then put under Ar flow with a wide glass exhaust.
4. Heat ODA to 300 °C and, and inject Se mixture. Let temperature return to 300 °C.
5. Inject 1.0 ml of Et_2Zn (10% by wt. in hexane) to the reaction flask and allow to react at 265 °C for around 3 min, or until the exciton absorbance peak shifts to a desired wavelength (λ=350-400 nm), upon which remove the flask from the heating mantle.
6. Once the temperature of the reaction flask drops to ~60 °C, add 12 ml methanol and split between two 15-ml centrifuge tubes, topping off with methanol. Centrifuge for 5 min and pour off the liquid phase. Redissolve the precipitated nanocrystals in toluene and repeat.

2. Growth of CdS Rods on ZnSe Cores[9]

1. Combine 3.0 g TOPO, 0.280 g ODPA, 0.080 g HPA, and 0.090 g CdO and add a magnetic stir bar in a three neck flask.
2. In a separate flask, combine 0.120 g S, and 4.0 ml TOP and add a magnetic stir bar.
3. Degas CdO solution for 45 min at 150 °C and TOP for 45 min at 120 °C, then put under Ar flow with wide glass exhausts.
4. Heat the CdO solution to 380 °C until CdO is dissolved and solution is clear and colorless. Meanwhile, heat the S solution to 120 °C until S is dissolved and the mixture is clear and colorless.
5. Add all of the ZnSe from step **1** to the S solution.
6. Add 2.0 ml of TOP to the Cd solution and let the temperature return to 380 °C. Once 380 °C is reached, immediately inject the S solution into the Cd solution.
7. Allow the nanorods to grow for 6-9 min, including the temperature recovery time, and remove the flask from the heating mantle. The longer the solution is left on the heat, the longer the rods will be.
8. Product may be a green gel, add chloroform to liquefy and split into two vials.
9. Precipitate nanocrystals in ethanol, pour off the liquid phase, and redissolve the precipitated nanocrystals in chloroform.

3. Growth of Pt Tip on CdS Rods[10]

1. Combine 0.2 ml OA, 0.2 ml oleylamine, 10 ml diphenyl ether, and 43 mg 1,2-hexadecanediol and add a magnetic stir bar in a flask.
2. Degas the mixture for 1 hr at 80 °C, then put under Ar flow and increase temp to 200 °C.
3. Add a mixture of CdS rods in chloroform and 20 mg Pt (II) acetylacetonate. After 5-7 min of the reaction mixture being at 190 °C, the solution will turn black. Remove the flask from the heat.
4. Precipitate nanocrystals in a 10:3 mixture of methanol to chloroform with a centrifuge and pour off the liquid phase. Redissolve the precipitated crystals in chloroform and repeat.

4. Ligand Exchange with MUA[11]

1. In a vial, disperse nanorods in 10 ml chloroform.
2. Add 0.1 g MUA to the nanorod solution and sonicate until all the MUA is dissolved.
3. In a separate vial, dissolve 0.1 g KOH in 20 ml triple distilled water (TDW).
4. Add approximately 5.0 ml of the TDW solution to the nanorod solution and shake vigorously.
5. Centrifuge the mixture from step 4.4 at 6000 rpm for 1 min to separate the aqueous and organic phases.
6. Collect the top (aqueous) phase and add methanol to achieve a solution that is 3:1 methanol to water.
7. Centrifuge the mixture from step 4.6 at 6000 rpm for 2 min to precipitate nanocrystals. Pour off the liquid phase and redisperse the precipitated crystals by sonicating in TDW.
8. If the organic phase in step 4.5 still retains some of the color of the original nanocrystal solution, repeat steps 4.4 through 4.7.

5. Synthesis of PbS Cores (Adapted from ref.[12])

1. Combine 0.49 g PbO, 18 ml ODE, and 1-16 ml OA (Depending on desired size, more OA yields larger particles) and add a magnetic stir bar in a three neck flask.
2. In a separate flask, add 10 ml ODE and a magnetic stir bar.
3. Degas both flasks for 1 hr at 120 °C, then put under Ar flow.
4. Heat the Pb solution to 135 °C. Meanwhile, cool the flask containing only ODE to room temperature.
5. Add 0.21 ml TMS to the room temperature ODE, then inject the mixture into the Pb solution at 135 °C.
6. Heat the mixture at 135 °C for 1-5 min (depending on desired size, longer heating yields larger particles), and place into an ice bath to quench the reaction.
7. Precipitate nanocrystals in distilled acetone, pour off the liquid phase, and redissolve precipitated crystals in toluene. Repeat two more times.

6. Growth of CdS Shell on PbS Cores[13]

1. Combine 1.0 g CdO, 6 ml OA, and 15 ml ODE and add a magnetic stir bar in a three neck flask.
2. In a separate flask add 20-40 mg of PbS cores dissolved in toluene and a magnetic stir bar.
3. Heat the CdO solution to 280 °C until the solution is clear and colorless, then cool to 100 °C.
4. Heat the PbS solution to 110 °C for no more than 5 min to boil off excess, but not all, solvent, then inject the Cd solution.
5. Slowly heat the reaction mixture to 120-160 °C (depending on the desired shell thickness). For thinner shells (1-2 monolayers) quench the reaction immediately after the injection of the Cd solution.
6. Once desired temperature is reached, quench the reaction by placing the flask in an ice bath.
7. Precipitate crystals in ethanol, pour off the liquid phase, and redissolve the precipitated crystals in toluene. Repeat twice. On final cleaning cycle, redissolve and store the crystals in anhydrous octane.

7. Preparation of TiO_2 on FTO/Glass Substrates

1. Hand wash the FTO coated glass with detergent (Alconox) and rinse with deionized water.
2. Sonicate the glass in methanol, acetone, then isoproponal, for 5 min each and dry with Ar flow.
3. Place the glass in a bath of 75 mM $TiCl_4$ in deionized water and heat (in air) for 30 min at 70 °C.
4. Rinse the glass with deionized water and dry with Ar, then heat (in air) at 450 °C for 1 hr and let cool to room temperature.

5. While the glass is cooling, dissolve TiO_2 Dyesol paste in terpinol in a 3:1 ratio by weight.
6. Place 3 drops of the TiO_2 mixture on the center of the FTO side of a dry glass slide that has been treated with $TiCl_4$ and spin for 6 sec at 700 rpm and 1 min at 2,000 rpm.
7. Anneal the slide in air at 450-500 °C until the film turns brown, then clear.

8. Spin Coating PbS/CdS into a Film

1. All spin coating steps are performed in an argon glovebox.
2. Place 4-5 drops of PbS/CdS in octane (10 mg/ml) onto a still slide from step **7** and let spread until the center begins to dry, then spin for 5 sec at 600 rpm then 15 sec at 2,500 rpm.
3. Place 10 drops of a 1:3 MPA:methanol solution on the slide, fully covering the surface, and spin for 5 sec at 600 rpm, then 15 sec at 2,500 rpm.
4. Wash surface with methanol by placing 10 drops on the slide and spinning for 5 sec at 600 rpm, then 15 sec at 2,500 rpm.
5. Wash surface with octane by same method as in step 8.4.
6. Repeat steps 8.2-8.5 for each subsequent layer of the film.
7. Anneal the film after every third layer at 150 °C for 15 min. The final film should have an absorbance near 1.5 at the wavelength of the peak of the NC.

9. Dip Coating PbS/CdS Films

1. Prepare a solution of 0.43 g cadmium acetate in 80 ml methanol in a beaker large enough to completely submerge the sample.
2. Prepare a solution of sodium sulfide nonahydrate ($Na_2S•9H_2O$) in 80 ml methanol in a beaker large enough to completely submerge the sample.
3. Submerge the sample for 1 min in the Cadmium bath, and rinse with methanol. Then submerge for 1 min in the Sulfer bath, and rinse with methanol.
4. Repeat step 9.3 until pores are filled (generally 4-8 times).
5. Anneal sample at 150 °C for 15 min.

10. Treating Films with CTAB[14]

1. Place 0.25 ml of CTAB, dissolved in methanol, at a concentration of 10 mg/ml, on film from step **9** and let sit for 1 min, then spin at 2,500 rpm for 30 sec.
2. Rinse slide with 10 drops of methanol and spin until dry.
3. Repeat 10.1 and 10.2 once.

11. Representative Results

The evolution of the absorption and emission spectra corresponding to ZnSe/CdS/Pt NCs during each step of the synthesis is tracked in **Figure 1**. It can be seen that **Figure 1b** expresses absorbance peaks at ~350 nm and ~450, characteristic of ZnSe and CdS respectively, and, most notably, now displays the onset of a FL peak at ~550 nm. This FL feature is a result of emissive excitonic decay across the ZnSe/CdS interface. This type II interdomain FL is then quenched by the growth of the Pt tip (**Figure 1c**), due to the rapid injection of the delocalized electron into the metal moiety. This ultra-fast charge separation enables the utilization of the electron for the photocatalytic reduction of water. Hydrophilic MUA ligands are then added to facilitate the removal of the hole from the ZnSe domain, increasing stability by inhibiting oxidation of the semiconductor core, allowing for the sustained reduction of solar H_2 (**Figure 2**). As a result of hole scavenging, the organic ligands become susceptible to photodegradation, but this can be simply mitigated by the addition of fresh ligands, as seen in **Figure 2**. Thus, the introduction of hydrophylic ligands not only render the NCs water soluble, but they also adjust the energetics of the system to protect the nanostructure at the cost of the inexpensive, easy to replace organic surfactants.

For PbS/CdS nanocrystal solids, **Figure 3a and 3b** shows a schematic of the fabrication process and the final device. **Figure 3c**, a TEM image of the core/shell nanocrystals, shows that the CdS infiltrates evenly around the PbS core. The nanocrystal solid is shown to be relatively free of pores in **Figure 3d**, an SEM image of the cross-section of a device. One result of the shell growth, that is observable, is a blueshift in both the absorbance and emission peaks. This shift is attributed to the PbS core shrinking as the Cd ions infiltrate further into the core, and can be seen in **Figure 4**. A large increase in the emission can also be seen in **Figure 4**, due to the enhanced quantum confinement provided by the CdS shell. The CdS layer not only increases the emission, it also protects the core, increasing the thermal stability of the solid, up to almost 200 °C, almost 50 °C higher than a PbS nanocrystal solid alone. Solar cells constructed using this nanocrystal solid architecture have not only shown better thermal stability, but have also been shown to have higher open circuit voltages (as high as 0.7 V) than the related organically linked films. These films have also shown a much higher tolerance to oxygen atmospheres, lasting for several days in normal atmospheric conditions with no degradation.

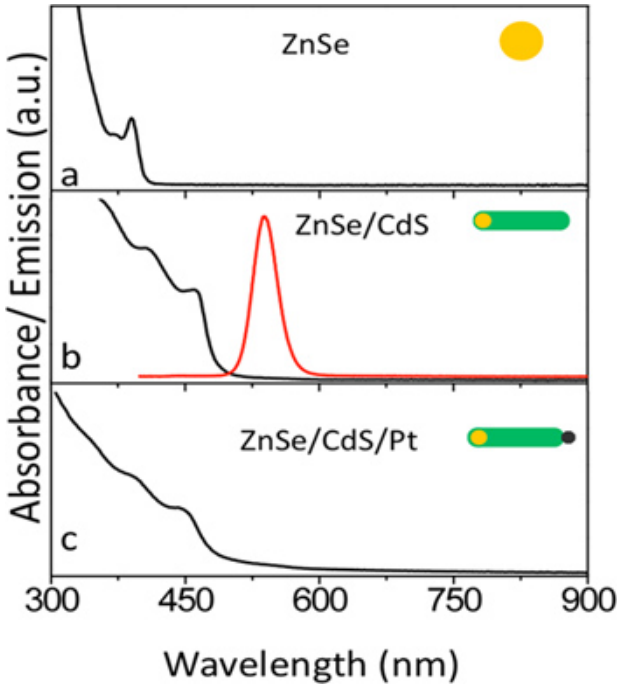

Figure 1. Optical properties of fabricated heteronanocrystals. (a). The absorbance of ZnSe NCs showing an excitonic feature at λ = 390 nm. Bandage emission was not observed for these samples. (b). Emission and absorbance of ZnSe/CdS nanorods grown from ZnSe core NCs. (c). Absorbance of ZnSe/CdS nanorods after Pt deposition.

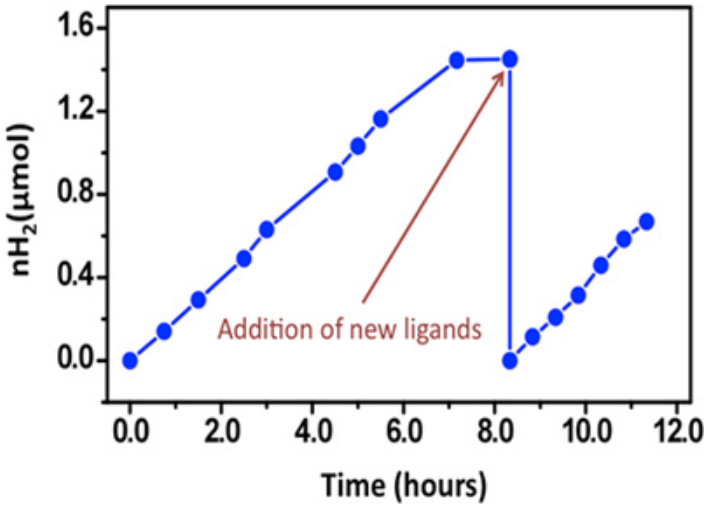

Figure 2. Evolution of hydrogen production on MUA capped ZnSe/CdS/Pt heteronanocrystals. The hydrogen production is resumed upon addition of new ligands to the ZnSe/CdS/Pt nanoparticles. The H2 production rate (the slope of the new experimental curve) after addition of fresh ligands (8-12 hr) is approximately the same as prior to the initial degradation (0-8 hr).

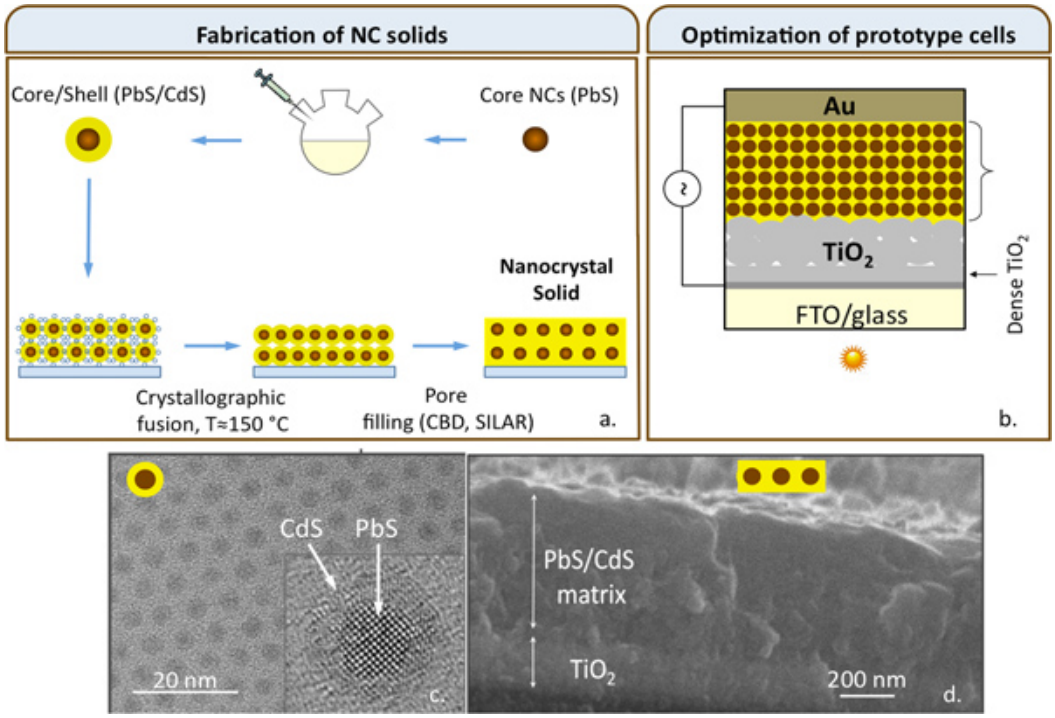

Figure 3. Schematic representation of (a) the steps involved in fabrication of Nanocrystal solids and (b) the final photovoltaic device. Below are SEM images of (c) PbS/CdS core/shell nanocrystals and (d) a side view of the nanocrystal solid.

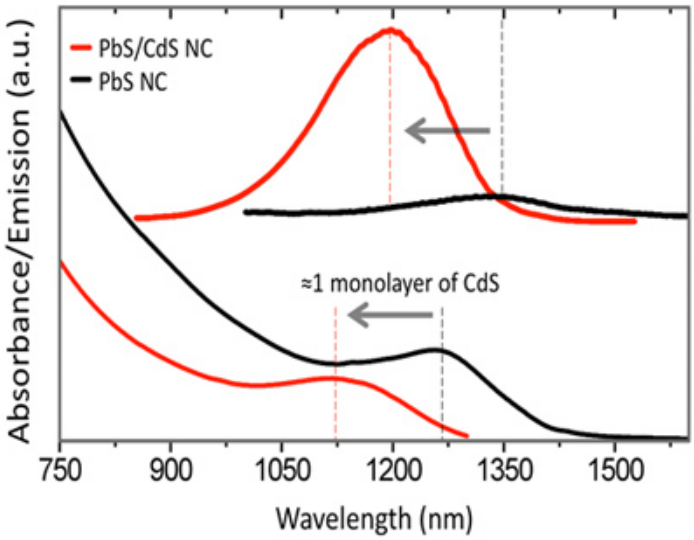

Figure 4. Changes in the absorption (bottom) and emission (top of PbS NCs resulting from the deposition of approximately 1 monolayer of the CdS shell. The shrinking of the PbS core from the cation exchange is reflected as a ≈150 nm shift in both spectra. The PbS fluorescence intensity is enhanced due to the formation of type 1 heterostructure.

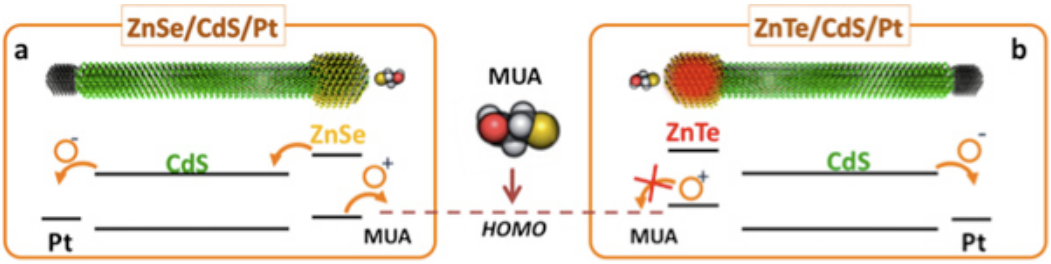

Figure 5. Schematic representation of energy level alignment in (a) ZnSe/CdS/Pt core/rod/tip structures and (b) ZnTe/CdS/Pt core/rod/tip structures. Choosing appropriate materials is of the utmost importance in these devices, as holes from ZnTe seeded structures sit in an energy level that makes traveling to the ligand unfavorable.

Discussion

This study demonstrates how composite architectures of inorganic nanocrystals can be employed to achieve a spatial separation of photoinduced charges. In particular, these composites allow fine-tuning of the distribution of charges across the two domains, which are then available to perform either photocatalytic or photovoltaic function. For instance, efficient photocatalysts can be made if donor and acceptor nanocrystal domains are built into a single nanoparticle. The energetics of such a system is shown in **Figure 5**. Meanwhile, stacking of donor- and acceptor nanocrystal films can lead to photovoltaic materials.

As an example of charge separating nanocrystals, ZnSe/CdS/Pt dot-in-a-rod metal tipped hetero-nanostructures were designed for the efficient splitting of H_2O. By fabricating a structure with an intrinsic linear potential gradient, we enable the spatial separation of charges such that electrons and holes become localized in the domains of Pt and ZnSe, respectively. The energy of the excited electron can then be employed for the photo-induced reduction of protons in water, while the hole is injected into the surfactant molecule, maintaining the functionality of the nanocrystal. In this configuration, the ligand degradation presents a limitation on the system performance. Therefore, fresh ligands must always be available for the H_2production to be sustained where excess ligands in the aqueous medium will automatically replace damaged ligands. We expect that the use of re-chargeable, electron-donating ligands may significantly improve the turnover numbers of photocatalytic composites utilizing charge-separating semiconductor hetero-interfaces. The device may potentially be improved by growing a thinner CdS shell over the ZnSe core, minimizing the barrier for the holes ejected from the ZnSe domain, or by choosing a surfactant with a slightly higher HOMO level, thereby making the ejection of holes from ZnSe more energetically favorable.

The nanocrystal solid procedure enables the assembly of nanocrystals into an all-inorganic inorganic film. This methodology is designed to overcome the key limitations of the ligand linked nanocrystal films, namely poor thermal and chemical stability of the ligand-nanocrystal system. This is done by encasing the nanocrystal array into a matrix of a wide-band gap semiconductor. Fabricated films exhibit good thermal stability, which is attributed to the heteroepitaxial structure of nanocrystal-matrix interfaces. Here, we employ a CdS matrix to encapsulate a PbS nanocrystal array, such that the quantum confinement of incorporated nanocrystals is preserved. The inter-nanocrystal spacing can be controlled via the thickness of the wide bandgap semiconductor shell, affecting the conductivity of the film. This allows for very different devices to be made from the same type of nanocrystal structure. Films with smaller inter-nanocrystal spacing show compelling light-harvesting performance in prototype solar cells, with efficiencies recorded as high as 2.3%. In theory a film with greater nanocrystal separation could be used for devices such as an infrared emitter, and other fluorescent solids. It is expected that the matrix-encapsulation approach could be extended to other type I semiconductor/matrix combinations to aid the "bottom-up" development of all-inorganic nanocrystal films showing more adjustable carrier mobility, quantum confinement of incorporated charges, and compelling air-stability.

Disclosures

No conflicts of interest declared.

Acknowledgements

We would like to acknowledge Dr. Felix Castellano (BGSU) and N. R. Neal for advice and valuable discussions. We gratefully acknowledge OBOR "Material Networks" program and Bowling Green State University for financial support. This work was partly supported by the NSF under Award CHE - 1112227.

References

1. Kamat, P.V., Flumiani, M., & Dawson, A. Metal - Metal and Metal - Semiconductor Composite Nanoclusters. *Colloids Surf. A.* **202**, 269-279 (2002).
2. Dawson, A. & Kamat, P.V. Complexation of Gold Nanoparticles with Radiolytically Generated Thiocyanate Radicals ((SCN)2-). *J. Phys. Chem. B.* **105**, 960-966 (2001).
3. Borensztein, Y., Delannoy, L., Djedidi, A., Barrera, R.G., & Louis, C. Monitoring of the Plasmon Resonance of Gold Nanoparticles in Au/TiO2 Catalyst under Oxidative and Reducing Atmospheres. *J. Phys. Chem. C.* **114**, 9008 (2010).
4. Acharya, K.P., Khnayzer, R.S., O'Connor, T., Diederich, G., Kirsanova, M., Klinkova, A., Roth, D., Kinder, E., Imboden, M., & Zamkov, M. The Role of Hole Localization in Sacrificial Hydrogen Production by Semiconductor-Metal Heterostructured Nanocrystals. *Nano Lett.* **11**, 2919 (2011).

5. Amirav, L. & Alivisatos, A.P. Photocatalytic Hydrogen Production with Tunable Nanorod Heterostructures. *J. Phys. Chem. Lett.* **1** (7), 1051-1054 (2010).
6. Pattantyus-Abraham, A.G., Kramer, I.J., Barkhouse, A.R., Wang, X., Konstantatos, G., Debnath, R., Levina, L., Raabe, I., & Nazeeruddin, M.K., Gratzel, M., & Sargent E.H. Depleted-Heterojunction Colloidal Quantum Dot Solar Cells. *ACS Nano.* **4** (6), 3374-3380 (2010).
7. Kinder, E., Moroz, P., Diederich, G., Johnson, A., Kirsanova, M., Nemchinov, A., O'Connor, T., Roth, D., & Zamkov, M. Fabrication of All-Inorganic Nanocrystal Solids through Matrix Encapsulation of Nanocrystal Arrays. *J. Amer. Chem. Soc.* **133** (50), 20488-20499 (2011).
8. Davide, C.P., Liberato, M., Lucia, C.M., Stefan, K., Cinzia, G., Marinella, S. & Angela, A. Shape and Phase Control of Colloidal ZnSe Nanocrystals. *Chem. Mater.* **17**, 1296-1306 (2005).
9. Carbone, L., Nobile, C., de Giorgi, M., Sala, F.D., Morello, G., Pompa, P., Hytch, M., Snoeck, E., Fiore, A., Franchini, I.R., Nadasan, M., Silvestre, A.F., Chiodo, L., Kudera, S., Cingolani, R., Krahne, R., & Manna, L. Synthesis and Micrometer-Scale Assembly of Colloidal CdSe/CdS Nanorods Prepared by a Seeded Growth Approach. *Nano Lett.* **7**, 2942-2950 (2007).
10. Habas, S.E., Yang, P., & Mokari, T. Selective Growth of Metal and Binary Metal Tips on CdS Nanorods. *J. Am. Chem. Soc.* **130** (11), 3294-3295 (2008).
11. Costi, R., Saunders, A.E., Elmalem, E., Salant, A., & Banin, U. Visible Light-Induced Charge Retention and Photocatalysis with Hybrid CdSe-Au Nanodumbbells. *Nano Lett.* **8** (2), 637-641 (2008).
12. Hines, M.A. & Scholes, G.D. Colloidal PbS Nanocrystals with Size-Tunable Near-Infrared Emission: Observation of Post-Synthesis Self-Narrowing of the Particle Size Distribution. *Adv. Mater.* **15** (21), 1844-1849 (2003).
13. Pietryga, J.M., Werder, D.J., Williams, D.J., Casson, J.L., Schaller, R.D., & Klimov, V.I. Utilizing the Lability of Lead Selenide to Produce Heterostructured Nanocrystals with Bright, Stable Infrared Emission. *J. Am. Chem. Soc.* **130** (14), 4879-4885 (2008).
14. Tang, J., Kemp, K.W., Hoogland, S., Jeong, K.S., Liu, H., Levina, L., Furukawa, M., Wang, X., Debnath, R., Cha, D., Chou, K.W., Fischer, A., Amassian, Ar., Asbury, J.B., & Sargent, E.H. Colloidal-quantum-dot photovoltaics using atomic-ligand passivation. *Nat. Mat.* **10**, 765-771 (2011).

